THE JOURNAL OF BIOLOGICAL CHEMISTRY VOL. 286, NO. 30, pp. 26595–26602, July 29, 2011

Regulation of F_0F_1-ATPase from *Synechocystis* sp. PCC 6803 by γ and ϵ Subunits Is Significant for Light/Dark Adaptation*[S]

Received for publication, February 23, 2011, and in revised form, May 2, 2011 Published, JBC Papers in Press, June 1, 2011, DOI 10.1074/jbc.M111.234138

Mari Imashimizu[‡], Gábor Bernát[§], Ei-Ichiro Sunamura[‡], Martin Broekmans[§], Hiroki Konno[‡], Kota Isato[‡], Matthias Rögner[§], and Toru Hisabori[‡1]

From the [‡]Chemical Resources Laboratory, Tokyo Institute of Technology, Nagatsuta 4259-R1-8, Midori-Ku, Yokohama 226-8503, Japan and [§]Department of Plant Biochemistry, Ruhr-University Bochum, 44780 Bochum, Germany

The γ and ϵ subunits of F_0F_1-ATP synthase from photosynthetic organisms display unique properties not found in other organisms. Although the γ subunit of both chloroplast and cyanobacterial F_0F_1 contains an extra amino acid segment whose deletion results in a high ATP hydrolysis activity (Sunamura, E., Konno, H., Imashimizu-Kobayashi, M., Sugano, Y., and Hisabori, T. (2010) *Plant Cell Physiol.* 51, 855–865), its ϵ subunit strongly inhibits ATP hydrolysis activity. To understand the physiological significance of these phenomena, we studied mutant strains with (i) a C-terminally truncated ϵ ($\epsilon_{\Delta C}$), (ii) γ lacking the inserted sequence ($\gamma_{\Delta 198-222}$), and (iii) a double mutation of (i) and (ii) in *Synechocystis* sp. PCC 6803. Although thylakoid membranes from the $\epsilon_{\Delta C}$ strain showed higher ATP hydrolysis and lower ATP synthesis activities than those of the wild type, no significant difference was observed in growth rate and in intracellular ATP level both under light conditions and during light-dark cycles. However, both the $\epsilon_{\Delta C}$ and $\gamma_{\Delta 198-222}$ and the double mutant strains showed a lower intracellular ATP level and lower cell viability under prolonged dark incubation compared with the wild type. These data suggest that internal inhibition of ATP hydrolysis activity is very important for cyanobacteria that are exposed to prolonged dark adaptation and, in general, for the survival of photosynthetic organisms in an ever-changing environment.

F_0F_1-ATP synthase is a ubiquitous membrane bound enzyme found in bacterial plasma membranes, inner membranes of mitochondria, and thylakoid membranes of chloroplasts and cyanobacteria. It catalyzes the synthesis of ATP from ADP and inorganic phosphate, at the expense of the electrochemical proton gradient across these membranes generated by respiratory or photosynthetic electron transport. ATP synthase also catalyzes the ATP hydrolysis reaction and can act as an ATP-driven proton pump.

Both the basic architecture and catalytic mechanism of the F_0F_1-ATP synthase remained highly conserved during evolution. The enzyme consists of two structurally and functionally distinct elements: F_0 and F_1 (1–3). The extrinsic, catalytic F_1 moiety is responsible for ATP synthesis and hydrolysis and has a subunit composition of $\alpha_3\beta_3\gamma\delta\epsilon$, with the catalytic sites predominantly located on the β subunits (4). The membrane-integral F_0 part is a proton channel, which spans the membrane, and has a subunit composition of ab_2c_{10-15}. The proton gradient formed across the membrane by respiratory or photosynthetic electron transport drives the rotation of the c-ring together with the $\gamma\epsilon$-subunits relative to the ab_2-$\alpha_3\beta_3\delta$ stator. Rotation of the $\gamma\epsilon$ spindle is thought to induce a series of conformational changes in the three β subunits that lead to ATP synthesis. In contrast, hydrolysis of ATP causes rotation of the $\gamma\epsilon$ axis with the c-ring in the opposite direction, resulting in proton translocation.

Based on the analysis of their amino acid sequences and molecular structures, both α and β subunits are well conserved in prokaryotes and eukaryotes, whereas γ and ϵ subunits have diversified considerably during evolution. This might be related to the fact that both γ and ϵ subunits play critical roles in regulation of the activity of the enzyme (5, 6). In comparison with bacterial or mitochondrial ATPases, the chloroplast F_1 (CF_1) γ subunit contains an additional inserted region of ~35 residues, within which two cysteine residues allow redox regulation of ATPase activity by disulfide bond formation/elimination (7–10). Notably, though containing a similar insertion, the γ subunit of cyanobacterial F_1 lacks nine amino acids therein, including the two regulatory cysteines (11).

The ϵ subunit is known to act as an intrinsic inhibitor of ATPase activity, and of its two structural domains, an N-terminal β sandwich and a C-terminal helix-turn-helix (12, 13), the latter is required for inhibition (14, 15), possibly via a large conformational change from a hairpin configuration (so-called "retracted" state) to an "extended" state (16, 17). Although the chloroplast ϵ subunit seems to inhibit ATPase activity more strongly than bacterial ϵ (15, 18), single molecule rotation analysis of an isolated $\alpha_3\beta_3\gamma$ subcomplex provided direct evidence that cyanobacterial ϵ subunit inhibits the rotation of γ (19). Within bacteria, the amino acid sequence of the ϵ subunit is well conserved, but anaerobic bacteria such as *Clostridium pasteurianum* and *Chlorobaculum tepidum* lack the C-terminal α helix (20). This alternative structure results in a weaker inhibition of the ATPase activity. Physiologically, the primary role of ATP synthase in these bacteria must be for maintenance of the

* This work was supported by the Ministry of Education, Culture, Sports, Science, and Technology of Japan (Grants-in-aid for Scientific Research on Priority Areas 18074002; to T. H.), the German Research Foundation (Deutsche Forschungsgemeinschaft, SFB 480, project C1 (to M. R.)), the German Federal Ministry of Education and Research (BMBF, project Bio-H_2 (to G. B. and M. R.)), and the European Union project Solar-H_2 (to M. B. and M. R.).

[S] The on-line version of this article (available at http://www.jbc.org) contains supplemental Methods and Figs. S1–S4.

[1] To whom correspondence should be addressed: Chemical Resources Laboratory, Tokyo Institute of Technology, Nagatsuta 4259-R1-8, Midori-Ku, Yokohama 226-8503, Japan. Tel.: 81-45-924-5234; Fax: 81-45-924-5268; E-mail: thisabor@res.titech.ac.jp.

transmembrane electrochemical potential by ATP hydrolysis, as opposed to ATP synthesis.

The most plausible explanation for which photosynthetic organisms have developed a down-regulation system for ATPase activity by γ and ε subunits is to prevent wasteful ATP hydrolysis, this providing a stable intracellular ATP level in darkness. However, this remains to be proven conclusively. Previously, we reported a γ mutant in the unicellular cyanobacterium *Synechocystis* sp. PCC 6803 (hereafter referred to as *Synechocystis*[2]), which lacks this inserted region ($\gamma_{\Delta 198-222}$) (21). Detailed analysis of this strain and single molecule experiments of the $\alpha_3\beta_3\gamma$ complex containing the same mutation within the γ subunit of *Thermosynechoccus elongatus* BP-1, indicated that the evolutionary insertion of an additional segment into the γ subunit enables the frequent lapse of the enzyme into an ADP-inhibition state (21); this apparently helps to maintain the cellular ATP level in the dark.

However, despite extensive research, the physiological role of ATPase inhibition by the ε subunit is not yet fully understood. In this study, we designed and characterized a C terminus-truncated ε mutant ($\epsilon_{\Delta C}$) in *Synechocystis*. Furthermore, to understand the physiological significance of ATPase regulation, we designed and characterized a *Synechocystis* double mutant combining both $\epsilon_{\Delta C}$ and $\gamma_{\Delta 198-222}$ strains. Our results are discussed in the context of cellular strategies to overcome environmental stress conditions such as long term darkness or very low light.

EXPERIMENTAL PROCEDURES

Growth Conditions—Cells of the glucose-tolerant strain of *Synechocystis* sp. PCC 6803 (22) were grown at 30 °C in liquid BG11 medium (23) with 10 mM HEPES-KOH (pH 7.4) under continuous illumination (white fluorescent light, 30 μmol photons·m^{-2}·s^{-1}) and bubbling with 1% (v/v) CO_2-enriched air. Alternatively, cultures were grown on 1.5% (w/v) BG11 agar plates (Agar BA-10, High Quality, Ina Food Industry Co., Nagano, Japan) supplemented with 0.3% (w/v) sodium thiosulfate.

Gene Constructs and Transformation of Synechocystis—Gene constructs for the inactivation of the *atpE* gene and deletion of its C-terminal region are shown in the supplemental information. Transformants of *Synechocystis* with plasmids containing the mutant *atpE* gene were selected on BG11 plates for spectinomycin (20 mg μl^{-1}) resistance. For the construction of an $\epsilon_{\Delta C}/\gamma_{\Delta 198-222}$ double mutant, a plasmid containing the mutant *atpC* gene was transformed into the $\epsilon_{\Delta C}$ strain. The resulting transformants were selected on BG11 plates for spectinomycin (20 mg μl^{-1}) and kanamycin (20 mg μl^{-1}) resistance. Because cyanobacteria have multiple copies of genomic DNA (24), transformants were subcultured several times to obtain fully segregated mutants with homogeneous mutation on all copies of genomic DNA. Complete segregation was confirmed by PCR.

Preparation of Thylakoid and Soluble Fractions—*Synechocystis* cells were harvested in the late log phase (1–2 × 10^8 cells ml^{-1}), washed with 20 mM Tricine-NaOH (pH 8.0) and suspended in suspension buffer (10 mM Tricine-KOH (pH 8.0), 10 mM $MgCl_2$, 5 mM NaH_2PO_4, 2.5 mM K_2HPO_4, 1 M glycine betaine) supplemented with 0.5 M mannitol, 100 μM PMSF, 1 mM 6-amino-*n*-caproic acid and 0.2% lysozyme; glycine betaine should stabilize ATP synthase of cyanobacterial thylakoid membranes (25). After a 1.5-h incubation at room temperature, cells were concentrated by centrifugation and resuspended in suspension buffer supplemented with 100 μM PMSF and 1 mM 6-amino-*n*-caproic acid. After cell disruption for two times by French press (140 megapascals), unbroken cells were removed by centrifugation (3000 × *g* for 10 min at 4 °C). The supernatant was centrifuged for 30 min (60,000 × *g*, 4 °C), with the remaining supernatant used as soluble fraction. Precipitated thylakoid membranes were suspended in the suspension buffer and the chlorophyll (Chl) concentration was determined according to Ref. 26.

SDS-PAGE and Immunoblot Analysis—Proteins from the cell extract were separated by SDS-PAGE on a 16% (w/v) polyacrylamide gel and stained with Coomassie Brilliant Blue G-250 (Wako, Osaka, Japan). Precision Plus Protein Standard (Bio-Rad) was used as a molecular weight marker.

Expression analysis of ATPase β and ε subunits was carried out according to Ref. 27 using polyclonal antibodies raised against recombinant proteins of both subunits. Antibodies against the β subunit were obtained with recombinant β from the thermophilic *Bacillus* PS3 ATPase, whereas antibodies against ε of *Synechocystis* ATPase were generated with a purified full-length His-tagged recombinant protein (His-ε) as antigen.

ATPase Activity Measurements—ATP hydrolysis was determined by the following assay: 0.1 mg Chl ml^{-1} thylakoid suspension in an assay containing 45 mM Tricine (pH 8.0) with various amounts of $MgCl_2$ and Na-ATP. After a 30-min dark incubation at 30 °C, the reaction was stopped by addition of 4% (w/v) cold trichloroacetic acid. As control, an identical assay was incubated for 30 min, followed by addition of cold trichloroacetic acid and thylakoids.

The concentration of inorganic phosphate was determined according to Ref. 28. Samples were mixed with 0.65 M sulfuric acid and 8.5 mM ammonium molybdate and incubated for 20 min at room temperature. After addition of 5.1 mM hydrazine sulfate, 0.3 M sulfuric acid, and 0.3 mM stannous chloride, samples were incubated for another 20 min, followed by measuring absorbance at 630 nm (Model 680 microplate reader, Bio-Rad Laboratories). Data points were fitted with a hyperbolic function.

Δ*pH Measurements*—Relative changes in the pH gradient across the thylakoid membrane of whole cells were determined by pH-sensitive fluorescence dye acridine yellow (AY) according to Ref. 29, using a Dual-PAM 100 system with DUAL-EAY and DUAL-DAY modules (Walz, Effeltrich, Germany) at an actinic light intensity of 120 μmol photons·m^{-2}·s^{-1} (30).

Electron Transport Rates (ETRs)—ETRs were derived from the steady-state (*F*) and maximal (F_m and F_m') chlorophyll fluorescence yield parameters recorded at defined light intensi-

[2] The abbreviations used are: *Synechocystis*, the unicellular cyanobacterium *Synechocystis* sp. PCC 6803; Tricine, *N*-[2-hydroxy-1,1-bis(hydroxymethyl)-ethyl]glycine; AY, acridine yellow; Chl, chlorophyll; $\epsilon_{\Delta C}$, C-terminally truncated ε mutant; ETR, electron transport rate; $\gamma_{\Delta 198-222}$, γ mutant lacking the inserted region (^{198}Leu–^{222}Val).

ties according to Ref. 31 in a Dual-PAM 100 system with Dual-E and DUAL-DR modules (30). Steady-state fluorescence yields were determined by rapid light curves with 30-s adaptation periods at stepwise-increased actinic light intensities from 0 to 250 μmol photons·m^{-2}·s^{-1}. Maximal fluorescence yields were obtained by saturating light pulses (duration, 600 s; intensity, 10,000 μmol photons·m^{-2}·s^{-1}) at the end of each 30-s period.

ATP Synthesis—ATP synthesis activity of thylakoid membranes (20 mg Chl ml^{-1}) was determined in an assay medium (40 mM Tricine-KOH (pH 8.0), 40 mM NaCl, 4 mM $MgCl_2$, 50 mM 1-methoxy phenazinium methyl sulfate, 2 mM Na_3PO_4, 40 mM diadenosine pentaphosphate, and 1 mM sodium ascorbate). For control experiments, the assay medium was supplemented with 50 mM carbonyl cyanide 4-(trifluoromethoxy) phenylhydrazone. After a 2-min dark incubation at 30 °C, 2 mM ADP was added, and ATP synthesis was induced by illumination. The ATP level was determined by a luciferin-luciferase assay according to Ref. 21.

Intracellular ATP Level Determination—ATP content in intact *Synechocystis* cells was determined according to Ref. 32. Erlenmeyer flask cultures in the late log phase ($1.5–2 \times 10^8$ cells ml^{-1}) were kept under either white light (40 μmol photons·m^{-2}·s^{-1}) or in the dark at 30 °C under continuous shaking (96 min^{-1}). Determination of the ATP level was carried out after mixing 50-ml aliquots with 2% (w/v) perchloric acid and neutralizing the supernatant with 1 M Tris-acetate (pH 7.5) (21).

RESULTS

F_oF_1 ε Subunit Is Essential for Growth of Synechocystis—To investigate the physiological role(s) of the F_0F_1 ε subunit, an ε knock-out mutant was constructed in *Synechocystis* (see supplemental Methods and Fig. S1*A*). However, the fact that only a partially segregated mutant could be achieved suggests that the ε subunit plays an essential role in cell viability. In a second approach, only the C-terminal domain of the ε subunit, critical for the inhibition of the ATPase activity (14, 15, 33), was removed by insertion of a stop codon (TAG) combined with insertion of a spectinomycin resistance cassette into the coding region of the *atpE* gene (supplemental Fig. S1*B*). As the amino acid sequence of the ε subunit is well conserved among bacteria (supplemental Fig. S2), the optimal position for the stop codon could be easily determined by using the crystal structure of the ε subunit of F_1 from the thermophilic *Bacillus* PS3 (TF_1) (34). This approach resulted in a completely segregated mutant strain consisting of a C-terminally truncated ε subunit ($\varepsilon_{\Delta C}$). Under continuous illumination, no significant difference in the color phenotype was observed between the WT and $\varepsilon_{\Delta C}$ mutant. Also, as revealed by SDS-PAGE analysis of the thylakoid membrane and soluble fraction (Fig. 1*A*), these strains did not differ in the composition of their major proteins.

Fig. 1, *B* and *C*, shows the immunoblot analysis using polyclonal antibodies raised against the TF_1-β subunit and His-tagged ε subunit, respectively. The identical amount of β subunit in WT and $\varepsilon_{\Delta C}$ strain suggests a similar amount of F_0F_1 in these cells (Fig. 1*B*). Immunoblotting with a His-ε antibody

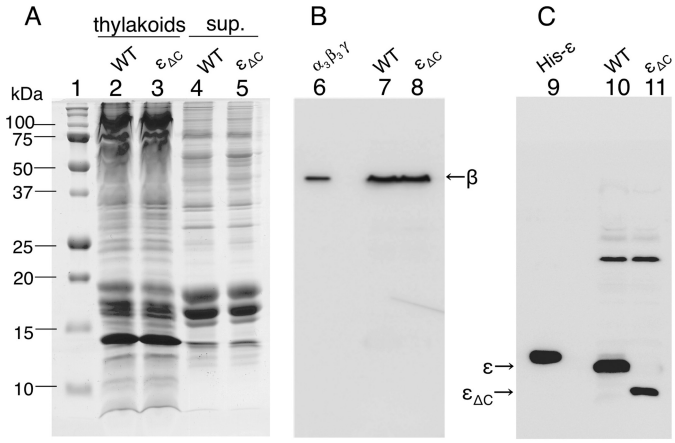

FIGURE 1. **SDS-PAGE and immunoblot analysis of cell extracts from WT and $\varepsilon_{\Delta C}$ *Synechocystis* strains.** *A*, SDS-PAGE of the thylakoid and supernatant (*sup.*) fractions stained by Coomassie Brilliant Blue G-250. Thylakoid (*lanes 2* and *3*) and supernatant fractions (*lanes 4* and *5*) contain 5 μg of Chl and 30 μg of protein, respectively. *Lane 1* shows the bands of the molecular mass marker. *B* and *C*, immunoblotting of ATPase β and ε subunit with rabbit polyclonal antibodies against TF_1-β protein and His_{10}-tagged ε protein overexpressed in *E. coli*. Purified recombinant $\alpha_3\beta_3\gamma$ complex and His-ε subunits were used as markers (*lanes 6* and *9*, respectively). Thylakoids (*lanes 7*, *8*, *10*, and *11*) contained 4 μg of Chl per lane.

shows one intense band and several weak bands with higher molecular mass in both the WT and $\varepsilon_{\Delta C}$ strain (Fig. 1*C*). Although the major band represents the ε subunit, the minor bands indicate other histidine-rich proteins which are anchored to the membrane. Although both the position and intensity of the mutant ε subunit was different from WT, the position of the C-terminally deleted ε subunit corresponds perfectly with the molecular mass of the truncated polypeptide. The lower intensity of this band is most likely due to a different affinity of truncated *versus* full-length ε subunit to the polyclonal antibody, rather than a lower amount of ε in the $\varepsilon_{\Delta C}$ strain.

Cyanobacterial F_oF_1 ε Subunit Inhibits ATPase Activity—Fig. 2*A* shows a comparison of ATP hydrolysis activities of isolated thylakoid membranes from WT and $\varepsilon_{\Delta C}$ strain in the dark. Although both strains showed very similar K_m values for ATP hydrolysis (WT, 140 μM; $\varepsilon_{\Delta C}$, 120 μM), the maximal ATPase activity of the $\varepsilon_{\Delta C}$ mutant was 2-fold or more higher than for the WT. This clearly indicates that the C-terminal domain of the ε subunit indeed impairs the cyanobacterial ATPase activity, whereas similar K_m values suggest a similar affinity of F_0F_1 for ATP, despite the deletion of the C-terminal domain of the ε subunit.

To investigate the impact of the $\varepsilon_{\Delta C}$ mutation on ATP synthesis, the activity of isolated thylakoid membranes from both WT and $\varepsilon_{\Delta C}$ strain was compared (Fig. 2, *B* and *C*). In both strains, ATP synthesis activity increased with increasing light intensity; under high light (200 μmol photons·m^{-2}·s^{-1}), activity of the WT and $\varepsilon_{\Delta C}$ mutant was 0.71 ± 0.29 and 0.36 ± 0.16 μmol ATP·mg Chl^{-1}·min^{-1} from the initial slope (Fig. 2*B*), respectively, and the corresponding activity under low light (50 μmol photons·m^{-2}·s^{-1}) was 0.51 ± 0.11 and 0.26 ± 0.09 μmol ATP·mg Chl^{-1}·min^{-1} (Fig. 2*C*).

Steady-state pH Gradient Is Low in Light-exposed $\varepsilon_{\Delta C}$ Cells—Fig. 3 shows the generation of the pH gradient across thylakoid

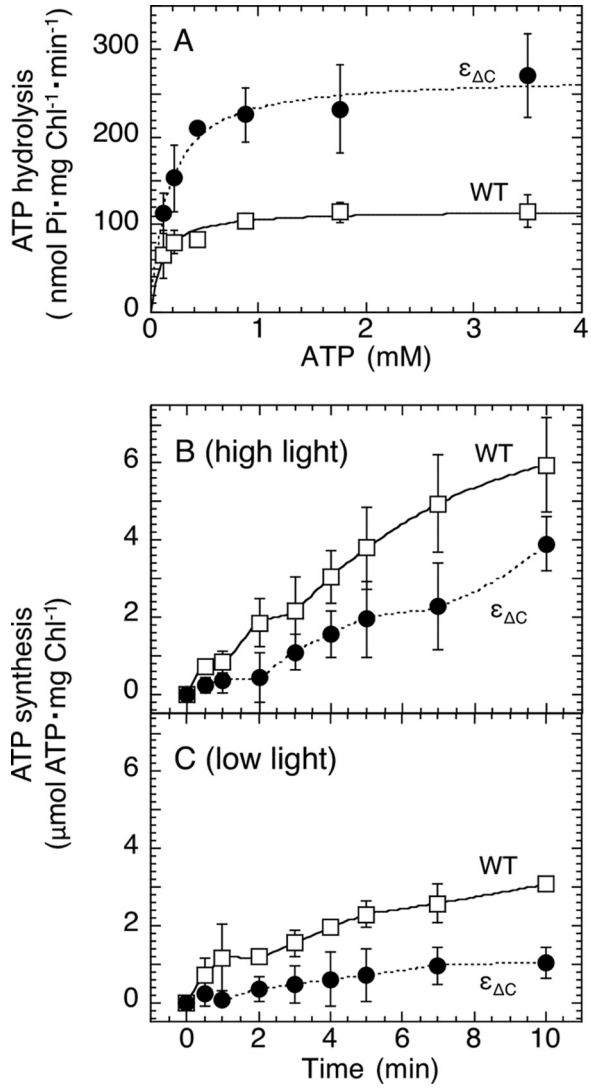

FIGURE 2. **ATP hydrolysis and ATP synthesis activity of thylakoid membranes from WT and $\epsilon_{\Delta C}$ strains.** *A*, ATP hydrolysis activity as monitored by colorimetric determination of inorganic phosphate (average of three independent measurements with S.D. except at 0.4 mM ATP representing the average of two). Experimental data were fitted with a hyperbolic function. *B* and *C*, ATP synthesis of WT and $\epsilon_{\Delta C}$ strain at two different light intensities: 200 μmol photons·m^{-2}·s^{-1} (*B*) and 50 μmol photons·m^{-2}·s^{-1} (*C*). The net amount of synthesized ATP was determined by subtracting the corresponding activities in the presence of 50 μM carbonyl cyanide 4-(trifluoromethoxy) phenylhydrazone (average of three independent measurements with S.D.). *Open squares*, WT; *filled circles*, $\epsilon_{\Delta C}$.

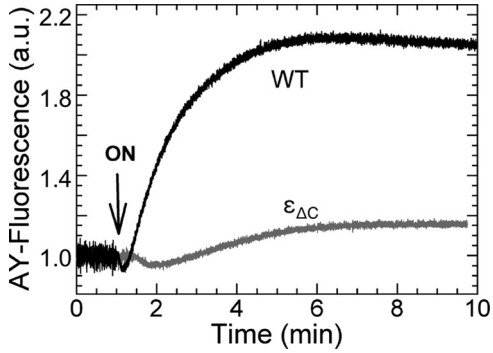

FIGURE 3. **Kinetics of ΔpH formation across thylakoid membranes.** Kinetics of actinic light-induced (*arrow*) ΔpH formation across thylakoid membranes followed by AY fluorescence in whole cells of WT and $\epsilon_{\Delta C}$ strains. For details and references, see under "Experimental Procedures." Upon illumination, the signal-to-noise level increases due to the high frequency modulation of the measuring beam. *Black line*, WT; *gray line*, $\epsilon_{\Delta C}$. *a.u.*, arbitrary unit.

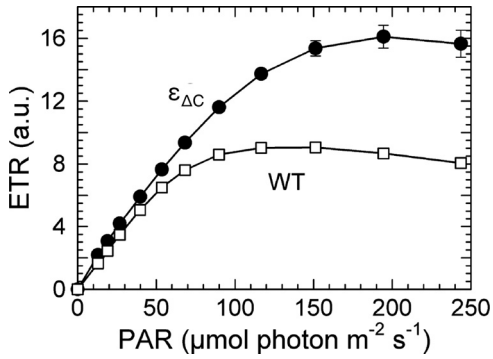

FIGURE 4. **Light saturation curves of the photosynthetic electron transport rates.** Light saturation curves of the photosynthetic ETRs in WT and $\epsilon_{\Delta C}$ strains were determined by chlorophyll *a* fluorescence measurements. For details and references, see under "Experimental Procedures." ETRs of five independent measurements were determined and averaged against photosynthetically active radiation (*PAR*); S.D. are shown as *error bars* (for the WT, the *error bars* are smaller than the symbol size). *Open squares*, WT; *filled circles*, $\epsilon_{\Delta C}$. *a.u.*, arbitrary unit.

membranes in intact cyanobacterial cells upon illumination as observed by the pH-sensitive fluorescence dye, AY (29). The relative increase in the AY fluorescence yield ($\Delta F/F$) was more than five times smaller in the $\epsilon_{\Delta C}$ strain than in the wild type. In addition, the kinetics of ΔpH formation was much slower in the mutant ($t_{1/2}$ = 2.8 *versus* 1.1 min).

High Electron Transport Rates in $\epsilon_{\Delta C}$ Cell Due to Low pH Gradient (Natural Uncoupling)—Fig. 4 shows photosystem II-mediated ETR in dependence of light intensity as determined by a chlorophyll fluorescence-based method (31). This so-called light saturation curve consists of a linear light-limited phase at low light and a photosynthesis-limited plateau at high light intensities. The initial slope (potential rate, α), the maximal ETR (ETR_{max}), and their crossing point ($I_k = \alpha/ETR_{max}$, the minimal saturating light intensity) provide a quantitative indication of the photosynthetic performance (*e.g.* Ref. 35). All three parameters (ETR_{max}, α, and I_k) are higher in the $\epsilon_{\Delta C}$ strain than in the WT; ETR_{max} in particular is almost twice as high as in the $\epsilon_{\Delta C}$ strain. In conclusion, the formation of a low steady-state pH gradient across thylakoid membranes in the mutant cells (Fig. 3) correlates with a high photosynthetic ETR. This phenomenon is similar to the uncoupled state of photosynthesis, when protonophores are used for measurement.

Growth of $\epsilon_{\Delta C}$ Strain Is Inhibited by High Light—Both under continuous illumination and under light-dark cycles, growth rates of WT and $\epsilon_{\Delta C}$ strain in liquid cultures are very similar (supplemental Fig. S3). However, *Synechocystis* cells often aggregate in liquid culture upon stress such as high light exposure, which decreases local light intensities and may dilute the impact of high light. For this reason, cell growth under low and high light conditions was also monitored on agar plates (supplemental Fig. S4). Although there was no difference in growth under low light, following a 4-day cultivation under high light, the $\epsilon_{\Delta C}$ strain showed significantly lower cell densities than the WT (supplemental Fig. S4, *A* and *B*), indicating an enhanced sensitivity of the $\epsilon_{\Delta C}$ strain for photodamage.

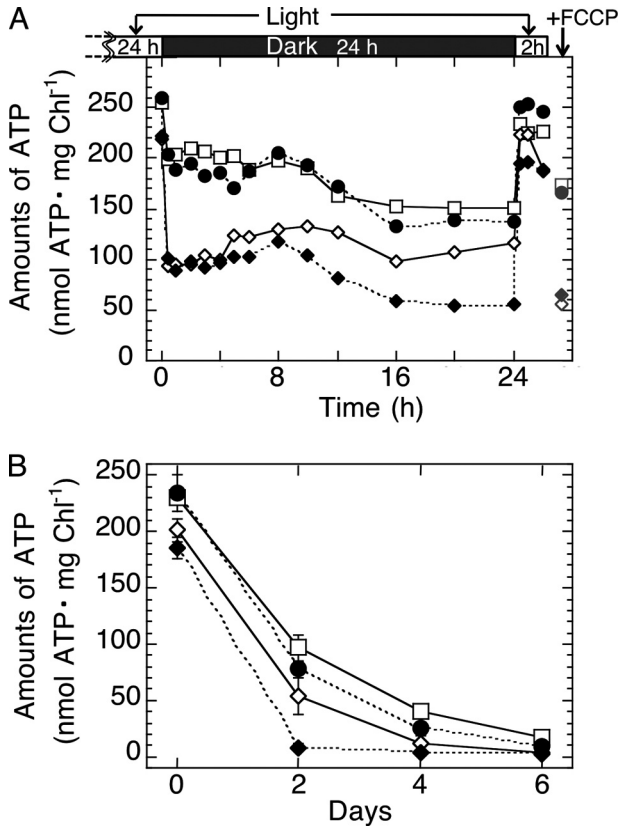

FIGURE 5. **Intracellular ATP levels after middle and long term dark incubation.** *A*, middle term (0–24 h) changes. After 24 h of continuous illumination, the light was turned off ($t = 0$), and cells were incubated in the dark for another 24 h. At the end of the dark period, the light was turned on again ($t = 24$ h), and ATP levels were also determined during the subsequent 2 h of light exposure. 50 μM carbonyl cyanide 4-(trifluoromethoxy) phenylhydrazone (*FCCP*) was added at the end of the experiment (*black arrow*); these data are shown as *gray symbols*. Each trace represents the average of two independent measurements. *Open squares*, WT; *filled circles*, $\epsilon_{\Delta C}$; *open diamonds*, $\gamma_{\Delta 198-222}$; *filled diamonds*, $\epsilon_{\Delta C}/\gamma_{\Delta 198-222}$. *B*, effect of long term dark adaptation (0–6 days) on the intracellular ATP level. Following 1 day of light adaptation (day 0, see *A*) cultures were dark adapted for 2, 4, or 6 days. Symbols as in *A*, with S.D. shown as *error bars* ($n = 3$).

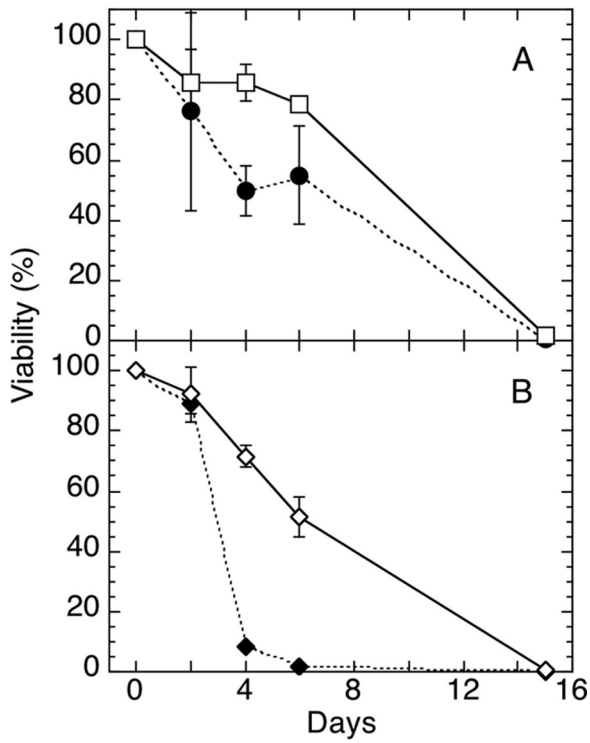

FIGURE 6. **Viability of WT and mutant strains after long term dark adaptation.** After 1 day of light adaptation (day 0) cultures were adapted in the dark for 2, 4, 6, or 15 days (*A* for WT and $\epsilon_{\Delta C}$ and *B* for $\gamma_{\Delta 198-222}$ and $\epsilon_{\Delta C}/\gamma_{\Delta 198-222}$ strains). Viabilities were determined by plating 5-fold serial dilutions of light and dark adapted cells on BG11 plates followed by 1 month of growth under low light condition (10 μmol photons·m^{-2}·s^{-1}). The number of colonies from the light adapted culture was defined as 100% in each strain. S.D. are shown as *error bars* ($n = 3$). *Open squares*, WT; *filled circles*, $\epsilon_{\Delta C}$; *open diamonds*, $\gamma_{\Delta 198-222}$; *filled diamonds*, $\epsilon_{\Delta C}/\gamma_{\Delta 198-222}$.

Inhibition of ATPase Activity Is Required for Maintaining Intracellular ATP Level under Prolonged Darkness—We previously reported a lower intracellular ATP level for a *Synechocystis* γ mutant ($\gamma_{\Delta 198-222}$) lacking the inserted region, especially in the dark (21). For further elucidation of the physiological role of the γ and ϵ subunits, we constructed a *Synechocystis* double mutant lacking both the C-terminal region of the ϵ subunit and the inserted region of γ subunit. Similar to the single deletion strains, this double mutant resembled the WT in growth rate and color phenotype, both under continuous illumination and under light-dark cycles in liquid cultures.

Fig. 5*A* shows the *in vivo* determination of the intracellular ATP level in WT and all three mutant strains under light and dark conditions. No significant differences were observed between the WT and $\epsilon_{\Delta C}$ strain, including the transient changes in the ATP level upon light on and off. Following transfer to dark, both strains showed an initial 25–30% drop in ATP level, which gradually decreased to ~55%. In contrast, ATP level in both $\gamma_{\Delta 198-222}$ mutant and $\epsilon_{\Delta C}/\gamma_{\Delta 198-222}$ double mutant decreased to only 80–85% of WT under illumination. Upon lights off, the ATP level dropped immediately below 50% in both strains but kept constant at this level for at least 24 h. Also, the ATP level in the $\gamma_{\Delta 198-222}$ strain kept constant at ~50%, whereas it gradually decreased in the double mutant to 25%. Upon lights on, the original ATP level was quickly restored in all strains. Also, addition of the protonophore carbonyl cyanide 4-(trifluoromethoxy) phenylhydrazone resulted in a drop in ATP level in all strains, as induced by light off.

Prolonged dark adaptation resulted in significant differences in the intracellular ATP level of WT and mutant strains (Fig. 5*B*). Following 2, 4, and 6 days of dark incubation, the intracellular ATP level decreased to 42, 17, and 7% for WT and 33, 11, and 4% for the $\epsilon_{\Delta C}$ strain, respectively. In the $\gamma_{\Delta 198-222}$ strain (27, 6, and 2%) and especially in the $\epsilon_{\Delta C}/\gamma_{\Delta 198-222}$ strain (4, 2, and 1%), the respective decay of the intracellular ATP level was even more pronounced.

Viabilities of WT and mutant strains after prolonged dark incubation are shown in Figs. 6, *A* and *B*. Although 2 days of dark incubation resulted in similar effects for all strains, viability of cells from all F_0F_1 mutants was much lower than the WT when cells were incubated for 4 days or longer in the dark. After 6 days of dark incubation, viability was 79% for WT cells, in comparison with 55 and 51% for $\epsilon_{\Delta C}$ and $\gamma_{\Delta 198-222}$ strains, respectively. With 2% viability after 6 days of dark incubation, a

more drastic effect was observed in the $\epsilon_{\Delta C}/\gamma_{\Delta 198-222}$ double mutant, whereas 15 days of dark incubation were required to achieve the same effect in the WT.

DISCUSSION

The inability to generate a fully segregated ε knock-out strain provides strong evidence that the F_0F_1 ε subunit is essential in *Synechocystis.* At the molecular level, there are two plausible explanations for this result. Firstly, deletion of the ε subunit may directly affect assembly of F_0F_1 in cyanobacteria. In ATPase from *Escherichia coli* and *Bacillus* PS3, the ε subunit is a prerequisite for binding F_1 to F_0, although F_1 from *E. coli* with a C-terminally truncated ε subunit is still able to bind to F_0 (36–39). In the green alga *Chlamydomonas reinhardtii*, even just partial deletion of the C-terminal part of ε affects F_0F_1 assembly (40); thus, the entire ε subunit seems to be required for this process (41). However, purified ε-depleted CF_1 from spinach can reconstitute with CF_1-depleted thylakoid membranes at high Mg^{2+} concentrations, indicating that the ε subunit may not be required for binding of CF_1 to CF_o under certain specific conditions (42). As F_0F_1-ATP synthase is essential for photophosphorylation and oxidative phosphorylation, a defect in the assembly of this enzyme would be expected to be lethal. The fact that in *Synechocystis*, the F_0F_1 expression level was not affected by the deletion of the ε subunit C-terminal domain (Fig. 1), indicates that in cyanobacteria the N-terminal β sandwich domain of this subunit is sufficient for proper assembly of F_0F_1.

A second possible explanation for the lethal phenotype of the ε knock-out is a dramatic change in the proton permeability of the thylakoid membrane brought about by the mutation. The ε subunit of spinach chloroplasts has been reported to be required for proton gating, which is in agreement with the observation that thylakoid membranes with ε-depleted CF_1 could not form a substantial proton gradient under illumination; this, in turn, prevented photophosphorylation (42–44). The fact that our $\epsilon_{\Delta C}$ *Synechocystis* strain showed the formation of a low pH gradient upon illumination (Fig. 3) and the ε knock-out mutant did not segregate suggests that the absence of the (entire) ε subunit results in an inability to synthesize ATP in cyanobacteria.

Under steady-state conditions, proton pumping from the cytoplasm to the lumen (proton influx) by photosynthetic and respiratory electron transport and by ATP hydrolysis must be balanced with the proton efflux due to ATP synthesis. This implies that changing any of these three processes strongly affects the steady-state pH gradient (29). The observed small increase in the AY fluorescence upon illumination as well as the slow kinetics in the mutant indicates a small impact of photosynthetic electron transport on the steady-state pH gradient on the one hand and a different balance of proton pumping and efflux on the other (see schematics on Fig. 7). These results are in accordance with the directly determined ATP synthesis and hydrolysis activities of thylakoid membranes isolated from WT and $\epsilon_{\Delta C}$ cells (Fig. 2).

To elucidate the relatively low impact of photosynthetic electron transport on the steady-state pH gradient in the $\epsilon_{\Delta C}$ strain and the modified balance of proton influx and efflux, direct ETR measurements were performed (Fig. 4). It could be expected that, particularly in the $\epsilon_{\Delta C}$ strain with higher ETR than WT, the linear electron flow under long term high light may exceed the CO_2 fixation capacities. This could result in photodamage by accumulation of reductants, and indeed, the $\epsilon_{\Delta C}$ mutant showed more sensitivity toward light stress (supplemental Fig. S4). Our results are also in agreement with data of *E. coli* showing that the C-terminal part of the ε subunit is required for efficient coupling of ATP synthesis/hydrolysis with proton pumping (39, 45). In conclusion, truncation of the ε subunit results in a "natural" uncoupling (*i.e.* without addition of any agent), which could potentially be used in biotechnology, *e.g.* in photobiological hydrogen production, where high linear ETR is required (46, 47).

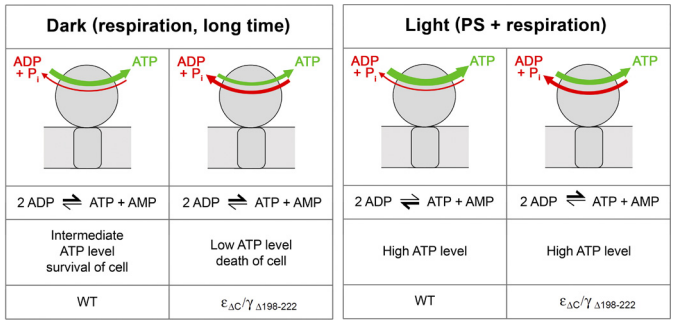

FIGURE 7. **ATP synthesis and hydrolysis coupled with photosynthesis and respiration in the cyanobacterial cell.** In the dark, ATP synthase in the $\epsilon_{\Delta C}$ mutant cell hydrolyze ATP, whereas the wild type cell can maintain ATP levels by oxidative phosphorylation. In the light, both the wild type and mutant cells can maintain high ATP levels.

Thylakoid membranes from the $\epsilon_{\Delta C}$ strain showed lower ATP synthesis rates during illumination than WT (Fig. 2, *B* and *C*; see also Fig. 7), which is probably due to the lower steady-state pH-gradient (Fig. 3). However, no significant difference was found for the intracellular ATP level of both strains under light conditions (Fig. 5). As the intracellular ATP level can also be affected by other enzymes such as adenylate kinase, the unchanged level of intracellular ATP in the mutant may result from compensatory up-regulation of this enzyme (48) and a shift in the 2ADP ⇆ ATP + AMP equilibrium depending on the intracellular AMP, ADP, and ATP levels (Fig. 7).

It is well known that the features of the ε subunit in the F_0F_1 complex show a considerable variety among organisms. Our results, obtained with the model cyanobacterium *Synechocystis* sp. PCC 6803, show that the C-terminal domain of the ε subunit plays an important role both for impairing ATP hydrolysis and for coupling proton translocation and ATP synthesis. Regulation of ATPase activity is likely to be important for photosynthetic organisms in the dark when the pH gradient across the thylakoid membrane is very small. No significant differences between the intracellular ATP level of WT and $\epsilon_{\Delta C}$ strain were observed even after 24 h of dark incubation, although the maximal ATPase activity of the $\epsilon_{\Delta C}$ mutant was ~2-fold higher than the WT (Figs. 5*A* and 2*A*, respectively; see also Fig. 7). Only after a prolonged dark incubation (Figs. 5*B* and 7), a difference in the intracellular ATP levels could be observed. These results are quite different from our previous observation showing that the intracellular ATP level in a *Synechocystis* strain with a mutated γ subunit, $\gamma_{\Delta 198-222}$, is dramatically decreased in the dark in

comparison with WT (21). Therefore, the physiological conditions under which ATPase inhibition via the ε subunit is required, are likely to be different from those for γ regulation.

Under dark aerobic conditions, ATP in cyanobacteria is mainly produced by oxidative phosphorylation and, to a smaller extent, by adenylate kinase (Fig. 7) (48). Due to these activities, the intracellular ATP level in WT and $\epsilon_{\Delta C}$ strain decreases only slightly during the first 8–10 h of dark incubation (Fig. 5*A*). As there is virtually no ATP production after this stage, prolonged dark adaptation (for 12 h or more) seems to induce a dormant state in unicellular cyanobacteria. Because the thermodynamic equilibrium of the F_0F_1-ATP synthase activity is shifted toward wasteful ATP hydrolysis at low pH gradients, most likely, the higher ATPase activity is responsible for the low intracellular ATP level in the $\epsilon_{\Delta C}$ mutant under prolonged dark incubation (Figs. 5*B* and 7). As could be shown for *Synechococcus elongatus* sp. PCC 7942, the expression of most genes is dramatically suppressed when cells are transferred from continuous illumination to complete darkness (49); this indicates that cellular metabolism is strongly affected by light/dark cycles in unicellular cyanobacteria. As the intracellular ATP level in *Synechocystis* (this study) could readily be regenerated by illumination, this suggests a substantial population of ATP synthases in the thylakoid membrane even under prolonged darkness.

Although cell viability was very similar between WT and the $\epsilon_{\Delta C}$ strains under normal light conditions (supplemental Fig. S4*A*), prolonged dark incubation resulted in a reduced viability of the $\epsilon_{\Delta C}$ mutant (Fig. 6*A*). Also, growth of the $\epsilon_{\Delta C}$ mutant was inhibited significantly under high light conditions (supplemental Fig. S4*B*), most probably due to its higher electron transport activity. The low cell viability of the $\epsilon_{\Delta C}$ mutant under prolonged dark incubation was most likely due to the lower intracellular ATP level as shown in Fig. 7, which summarizes the key findings and conclusions relating to this mutant.

The *Synechocystis* double mutant $\epsilon_{\Delta C}/\gamma_{\Delta 198-222}$, lacking both the ε C terminus and the inserted region of γ, showed similar transient changes in the intracellular ATP as the WT during a 24-h dark period, although at a lower ATP level (Fig. 5*A*). The much faster decrease in the intracellular ATP level during prolonged dark incubation in the double mutant as compared with WT or single mutant strains indicates that both γ and ε subunits of cyanobacterial F_1 play a critical role in preventing wasteful ATP hydrolysis. The double mutant also showed decreased cell viability under prolonged dark incubation compared with other strains (Fig. 6), presumably a consequence of the dramatic decrease in the intracellular ATP level.

In summary, inhibition of the ATPase activity of cyanobacterial F_0F_1-ATP synthase is key for maintaining the intracellular ATP level and for survival during prolonged dark intervals, to which cyanobacteria are frequently exposed in nature. By this, we can show that this regulatory system of the ATP synthase has a physiological impact on photosynthetic organisms. Indeed, for this down-regulation, the F_1 subunits γ and ε play a critical role, with γ likely playing a more dominant role. For an even better understanding of the physiological role of ε, determination of the conformational states of this subunit *in vivo* is mandatory.

Acknowledgments—We thank M. Yoshida for helpful discussions and valuable suggestions. We are also grateful for fruitful collaboration with Nadine Waschewski, Benjamin Bailleul, Conrad Mullineaux, and Ulrich Schreiber and acknowledge the excellent technical assistance of Erdmut Thomas.

REFERENCES

1. Boyer, P. D. (1997) *Annu. Rev. Biochem.* **66,** 717–749
2. Noji, H., Yasuda, R., Yoshida, M., and Kinosita, K., Jr. (1997) *Nature* **386,** 299–302
3. Yoshida, M., Muneyuki, E., and Hisabori, T. (2001) *Nat. Rev. Mol. Cell Biol.* **2,** 669–677
4. Yoshida, M., Sone, N., Hirata, H., Kagawa, Y., and Ui, N. (1979) *J. Biol. Chem.* **254,** 9525–9533
5. Hisabori, T., Ueoka-Nakanishi, H., Konno, H., and Koyama, F. (2003) *FEBS Lett.* **545,** 71–75
6. Frasch, W. D. (1994) in *The Molecular Biology of Cyanobacteria* (Bryant, D. A., ed.) pp. 361–380, Springer, Dordrecht, The Netherlands
7. Arana, J. L., and Vallejos, R. H. (1982) *J. Biol. Chem.* **257,** 1125–1127
8. Nalin, C. M., and McCarty, R. E. (1984) *J. Biol. Chem.* **259,** 7275–7280
9. Dann, M. S., and McCarty, R. E. (1992) *Plant Physiol.* **99,** 153–160
10. Kim, Y., Konno, H., Sugano, Y., and Hisabori, T. (2011) *J. Biol. Chem.* **286,** 9071–9078
11. Werner, S., Schumann, J., and Strotmann, H. (1990) *FEBS Lett.* **261,** 204–208
12. Wilkens, S., Dahlquist, F. W., McIntosh, L. P., Donaldson, L. W., and Capaldi, R. A. (1995) *Nat. Struct. Biol.* **2,** 961–967
13. Yagi, H., Konno, H., Murakami-Fuse, T., Isu, A., Oroguchi, T., Akutsu, H., Ikeguchi, M., and Hisabori, T. (2010) *Biochem. J.* **425,** 85–94
14. Kuki, M., Noumi, T., Maeda, M., Amemura, A., and Futai, M. (1988) *J. Biol. Chem.* **263,** 17437–17442
15. Nowak, K. F., and McCarty, R. E. (2004) *Biochemistry* **43,** 3273–3279
16. Tsunoda, S. P., Rodgers, A. J., Aggeler, R., Wilce, M. C., Yoshida, M., and Capaldi, R. A. (2001) *Proc. Natl. Acad. Sci. U.S.A.* **98,** 6560–6564
17. Kato-Yamada, Y., Yoshida, M., and Hisabori, T. (2000) *J. Biol. Chem.* **275,** 35746–35750
18. Weber, J., Dunn, S. D., and Senior, A. E. (1999) *J. Biol. Chem.* **274,** 19124–19128
19. Konno, H., Murakami-Fuse, T., Fujii, F., Koyama, F., Ueoka-Nakanishi, H., Pack, C. G., Kinjo, M., and Hisabori, T. (2006) *EMBO. J.* **25,** 4596–4604
20. Das, A., and Ljungdahl, L. G. (2003) *J. Bacteriol.* **185,** 5527–5535
21. Sunamura, E., Konno, H., Imashimizu-Kobayashi, M., Sugano, Y., and Hisabori, T. (2010) *Plant Cell Physiol.* **51,** 855–865
22. Williams, J. G. (1988) *Methods Enzymol.* **167,** 766–778
23. Stanier, R. Y., Kunisawa, R., Mandel, M., and Cohen-Bazire, G. (1971) *Bacteriol. Rev.* **35,** 171–205
24. Labarre, J., Chauvat, F., and Thuriaux, P. (1989) *J. Bacteriol.* **171,** 3449–3457
25. Mamedov, M. D., Hayashi, H., Wada, H., Mohanty, P. S., Papageorgiou, G. C., and Murata, N. (1991) *FEBS Lett.* **294,** 271–274
26. Grimme, L. H., and Boardman, N. K. (1972) *Biochem. Biophys. Res. Commun.* **49,** 1617–1623
27. Hishiya, S., Hatakeyama, W., Mizota, Y., Hosoya-Matsuda, N., Motohashi, K., Ikeuchi, M., and Hisabori, T. (2008) *Plant Cell Physiol.* **49,** 11–18
28. Fiske, C. H., and Subbarow, Y. (1925) *J. Biol. Chem.* **66,** 375–400
29. Teuber, M., Rögner, M., and Berry, S. (2001) *Biochim. Biophys. Acta.* **1506,** 31–46
30. Xu, M., Bernát, G., Singh, A., Mi, H., Rögner, M., Pakrasi, H. B., and Ogawa, T. (2008) *Plant Cell Physiol.* **49,** 1672–1677
31. Genty, B., Briantais, J. M., and Baker, N. R. (1989) *Biochim. Biophys. Acta* **990,** 87–92
32. Ohta, Y., Yoshioka, T., Mochimaru, M., Hisabori, T., and Sakurai, H. (1993) *Plant Cell Physiol.* **34,** 523–529
33. Xiong, H., Zhang, D., and Vik, S. B. (1998) *Biochemistry* **37,** 16423–16429
34. Yagi, H., Kajiwara, N., Tanaka, H., Tsukihara, T., Kato-Yamada, Y., Yoshida, M., and Akutsu, H. (2007) *Proc. Natl. Acad. Sci. U.S.A.* **104,** 11233–11238

35. Schreiber, U. (2004) in *Chlorophyll Fluorescence: A Signature of Photosynthesis* (Papageorgiou, G. C., and Govindjee, eds.) pp. 279–319, Springer, Dordrecht, The Netherlands
36. Yoshida, M., Okamoto, H., Sone, N., Hirata, H., and Kagawa, Y. (1977) *Proc. Natl. Acad. Sci. U.S.A.* **74,** 936–940
37. Sternweis, P. C. (1978) *J. Biol. Chem.* **253,** 3123–3128
38. Klionsky, D. J., and Simoni, R. D. (1985) *J. Biol. Chem.* **260,** 11200–11206
39. Cipriano, D. J., and Dunn, S. D. (2006) *J. Biol. Chem.* **281,** 501–507
40. Robertson, D., Boynton, J. E., and Gillham, N. W. (1990) *Mol. Gen. Genet.* **221,** 155–163
41. Johnson, E. A. (2008) *Photosynth. Res.* **96,** 153–162
42. Patrie, W. J., and McCarty, R. E. (1984) *J. Biol. Chem.* **259,** 11121–11128
43. Richter, M. L., Patrie, W. J., and McCarty, R. E. (1984) *J. Biol. Chem.* **259,** 7371–7373
44. Nowak, K. F., Tabidze, V., and McCarty, R. E. (2002) *Biochemistry* **41,** 15130–15134
45. Feniouk, B. A., Suzuki, T., and Yoshida, M. (2006) *Biochim. Biophys. Acta* **1757,** 326–338
46. Bernát, G., Waschewski, N., and Rögner, M. (2009) *Photosynth. Res.* **99,** 205–216
47. Waschewski, N., Bernát, G., and Rögner, M. (2010) *Biomass and Biofuels* (Vertès, A. A. G., Qureshi, N., Blaschek, H. P., and Yukawa, H., eds.) pp. 388–401, Wiley-Blackwell, Oxford
48. Bottomley, P. J., and Stewart, W. D. (1976) *Arch. Microbiol.* **108,** 249–258
49. Ito, H., Mutsuda, M., Murayama, Y., Tomita, J., Hosokawa, N., Terauchi, K., Sugita, C., Sugita, M., Kondo, T., and Iwasaki, H. (2009) *Proc. Natl. Acad. Sci. U.S.A.* **106,** 14168–14173